A Combined Theoretical and Experimental Study of Simple Terminal Group 6 Nitride and Phosphide N≡MX_3 and P≡MX_3 Molecules

Xuefeng Wang and Lester Andrews*

Department of Chemistry, University of Virginia, Charlottesville, Virginia 22904-4319

Roland Lindh, Valera Veryazov, and Björn O. Roos

Department of Theoretical Chemistry, Chemical Center, University of Lund, POB 124, 2-221 00 Lund, Sweden

Received: May 20, 2008

Organometallic complexes containing terminal metal nitrides and phosphides are important synthetic reagents. Laser-ablated group 6 metal atoms react with NF_3, PF_3, and PCl_3 to form the simple lowest energy N≡MF_3, and P≡MX_3 products following insertion and halogen transfer, with the exception of P≡CrF_3, which is a higher energy species and is not observed. The E≡MX_3 pnictide metal trihalide molecules are identified from both argon and neon matrix infrared spectra and frequencies calculated by density functional theory and multiconfigurational second-order perturbation theory (CASSCF/CASPT2). These simple terminal nitrides involve strong triple bonds, which range from 2.80 to 2.77 to 2.59 natural bond order for M = W, Mo, and Cr, respectively, as computed by CASSCF/CASPT2, and the M≡N stretching frequencies also follow this order. The terminal phosphides are weaker with bond orders 2.74, 2.67, and 2.18, respectively, as the more diffuse 3p orbitals are less effective for bonding to the more compact metal valence d orbitals.

Introduction

There is an extensive organometallic chemistry of complexes containing terminal metal nitride and phosphide functional groups. As expected, nitrides of the heavier transition metals came first, but phosphide research has accelerated recently.[1,2]

Such complexes with group 6 metals and terminal triple bonds are of particular interest here. Catalytic nitrile metathesis has been investigated for L_3MoN and L_xWN systems by the Johnson group.[3–5] Other relevant trialkoxide stabilized molecules with terminal nitride triple bonds and the ternary $WNCl_3$ compound have been characterized.[6,7] These ideas have been extended to terminal phosphide functional groups by Cummins and co-workers to investigate and employ alkoxide stabilized Mo≡P triple bonds, phosphaalkynes as metathesis reagents, and terminal nitride-to-phosphide conversions.[8–12] The foregoing chemistry involves mostly W and Mo pnictide triple bonds, but there are several examples of terminal chromium(VI) nitrido complexes.[13–15] However, the analogous complexes containing a chromium−phosphorus triple bond have not been prepared.

Chemistry of the group 6 metals Cr, Mo, and W in organometallic complexes provides interesting contrasts.[16,17] Because different d orbitals participate in bonding, tungsten and molybdenum compounds favor higher oxidation states whereas chromium counterparts tend to prefer lower oxidation states. However, a recent investigation of group 6 metal atom reactions with tri- and tetrahalomethanes produced the methylidyne molecules HC≡MX_3 and XC≡MX_3 with metal−carbon triple bonds.[18] These simple methylidyne molecules provide models for the larger alkylidyne complexes that are important in synthetic organometallic chemistry.[16] We report here an analogous combined experimental and theoretical investigation of the group 6 E≡MX_3 molecules and a comparison of the triple bonds formed with different pnictides, metals and halogens.

* Author for correspondence. E-mail: lsa@virginia.edu.

Experimental and Computational Methods

Laser ablated Cr, Mo and W atoms (Johnson-Matthey) were reacted with NF_3 (Matheson), PF_3 (PCR Research), and PCl_3 (Aldrich) in excess argon or neon during condensation at 4 K using a closed-cycle refrigerator (Sumitomo Heavy Industries Model RDK 205D) as described elsewhere.[19,20] Reagent gas mixtures were typically 0.2 or 0.4% in neon or argon. After reaction, infrared spectra were recorded at a resolution of 0.5 cm^{-1} using a Nicolet 750 spectrometer with an Hg−Cd−Te B range detector. Samples were later irradiated for 15 min periods by a mercury arc street lamp (175 W) with the globe removed using a combination of optical filters, and then samples were annealed to allow reagent diffusion and further reaction.

CASSCF and CASPT2 calculations were performed for all subject molecules.[25,26] The basis set was of VTZP quality with the primitives obtained from the relativistic ANO-RCC basis sets: 5s4p2d1f for P, 4s3p2d1f for F and N, and 6s5p3d2f1g for Cr, 7s6p4d2f1g for Mo and 9s8p6d4f2g1h for W.[27–29] Scalar relativistic effects are included in the calculations using the Douglas−Kroll−Hess Hamiltonian as is standard in the MOLCAS software. The active space was chosen to describe the M≡P and M≡N triple bonds: six active orbitals (three bonding and three antibonding) with six active electrons. However, for N≡CrF_3 a full valence active space was used because of the less ionic character of the Cr−F bond (12 electrons in 12 orbitals). All valence electrons, plus the semicore electrons 3s,3p for Cr, 4s, 4p for Mo, 5s, 5p for W, were correlated in the CASPT2 calculations, which used the standard IPEA Hamiltonian and an imaginary shift of 0.1 to remove some weak intruder states. All calculations were performed with the MOLCAS-7 quantum chemistry software.[30] The geometries were optimized at the CASPT2 level and vibrational frequencies were computed using numerical gradients and Hessians. All calculations were performed in C_s symmetry but all molecules converged to C_{3v} symmetry.

10.1021/jp804469a CCC: $40.75
Published on Web 08/12/2008

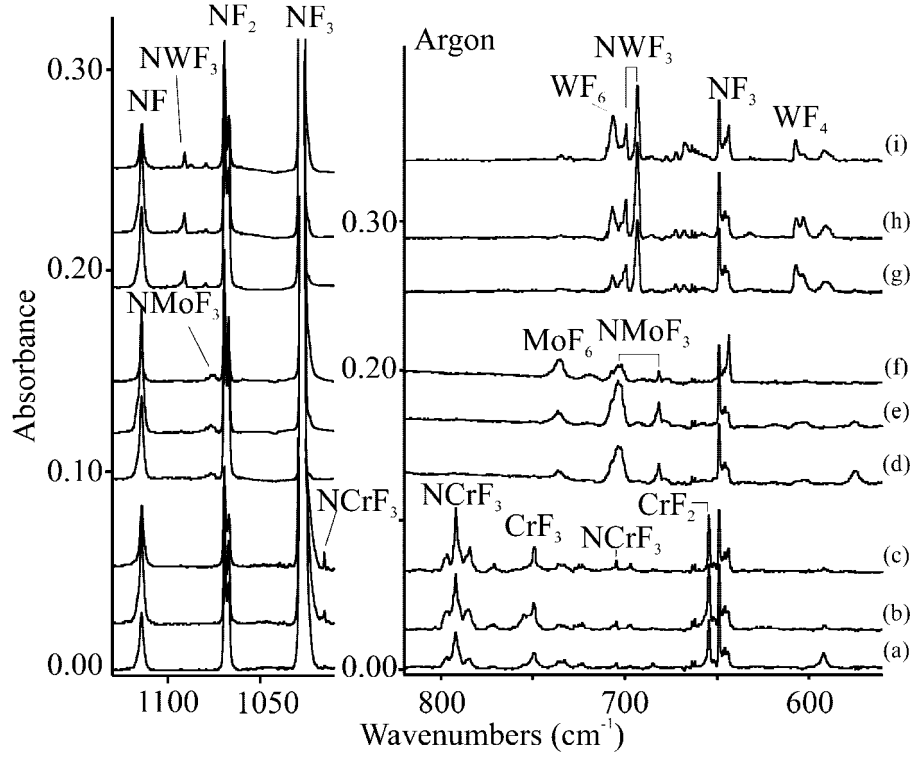

Figure 1. Infrared spectra for group 6 metal atom reaction products with NF_3 in excess argon in the 1130−1010 and 820−570 cm^{-1} regions: (a) spectrum after codeposition of laser-ablated Cr and NF_3 at 0.5% in argon at 4 K for 60 min, (b) after > 220 nm irradiation for 20 min, and (c) after annealing to 25 K; (d) spectrum after codeposition of laser-ablated Mo and NF_3 at 0.5% in argon at 4 K for 60 min, (e) after > 220 nm irradiation, and (f) after annealing to 25 K; (g) spectrum after codeposition of laser-ablated W and NF_3 at 0.5% in argon at 4 K for 60 min, (h) after > 220 nm irradiation for 20 min, and (i) after annealing to 25 K.

TABLE 1: Observed and Calculated Vibrational Frequencies of the Group 6 N≡MF$_3$ Molecules in Singlet Ground Electronic States with C_{3v} Structures[a]

approximate	N≡CrF$_3$							N≡MoF$_3$							N≡WF$_3$						
description	obs[b]	cal(L)	int	cal(W)	int	cal(C)	int	obs[b]	Cal(L)	int	cal(W)	int	cal(C)	int	obs[b]	cal(L)	int	cal(W)	int	cal(C)	int
M≡N, a_1	1015	1224	51	1162	46	1031	14	1075	1155	57	1110	50	1095	24	1091	1137	49	1098	40	1102	21
M−F, e	792	799	352	774	294	824	528	704	707	294	693	296	720	474	693	686	270	672	242	704	356
M−F, a_1	705	712	42	683	33	751	78	682	675	47	657	39	699	74	699	685	47	668	39	709	67
F−M−F, e		371	0	358	2	356	0		324	6	318	6	326	6		321	10	315	10	322	10
F−M−F,a_1 a		276	7	267	5	280	25		222	10	229	7	228	21		214	8	210	5	219	15
N−M−F, e		205	10	198	8	207	11		173	18	162	14	169	30		172	18	170	14	167	29

[a] Frequencies and intensities are in cm^{-1} and km/mol. Frequencies and intensities computed with B3LYP(L), BPW91(W), or CASSCF/CASPT2(C) methods in the harmonic approximation. Symmetry notations are for C_{3v} symmetry. [b] Observed in an argon matrix: the instrumental limit is 410 cm^{-1}. Neon matrix counterparts are (Cr) 1020, 798, 709 cm^{-1}, (Mo) 1080, 708, 688 cm^{-1}, and (W) 1096, 704, 699 cm^{-1}.

Complementary density functional theory (DFT) calculations were also carried out as done for analogous systems[17,18] using the Gaussian 03 package,[21] the B3LYP and BPW91 density functionals,[22] the 6-311++G(3df,3pd) basis sets for N, P, F and Cl[23] and the SDD pseudopotential and basis set for the metal atoms[24] to provide a consistent set of vibrational frequencies for the reaction products. Different spin states were computed to locate the ground-state product molecules. Geometries were fully relaxed during optimization, and the optimized geometry was confirmed by vibrational analysis. All of the vibrational frequencies were calculated analytically with zero-point energy included for the determination of reaction energies.

Results and Discussion

The reaction products of Cr, Mo and W atoms with EX_3 molecules will be characterized by matrix infrared spectra and quantum chemical calculations, and comparison to results from the analogous halomethane reactions.[17,18] These experiments also produce common absorptions due to precursor fragment reactive species such as NF, NF_2, NF_2^+, NF_2^-, PF_2, PF_2^+, PF_3^- and PCl_2 that have been reported previously.[31]

NF_3. Infrared spectra of the laser-ablated Cr, Mo, and W atom reaction products with NF_3 in excess argon are compared in Figure 1 and Table 1. For chromium, strong and weak new absorptions were observed at 1015.1, 791.9 and 704.7 cm^{-1}. These bands, marked as $NCrF_3$, increased in concert on sequential UV irradiation (>320 nm, 240−380 nm, then > 220 nm, only the latter illustrated) and sharpened on annealing to 25 K. Sharp bands at 654.3 and 749.4 cm^{-1} are due to CrF_2 and CrF_3 based on previous work[32] and their observation as weaker bands in the PF_3 experiments that follow. For molybdenum, a weak structured band at 1075 cm^{-1}, a strong, structured 704 cm^{-1} absorption, and a sharp 681.8 cm^{-1} band were observed. Ultraviolet irradiation increased these bands slightly, and they decreased on subsequent annealing. In addition a weak 736.8, 734.9 cm^{-1} band increases more on photolysis

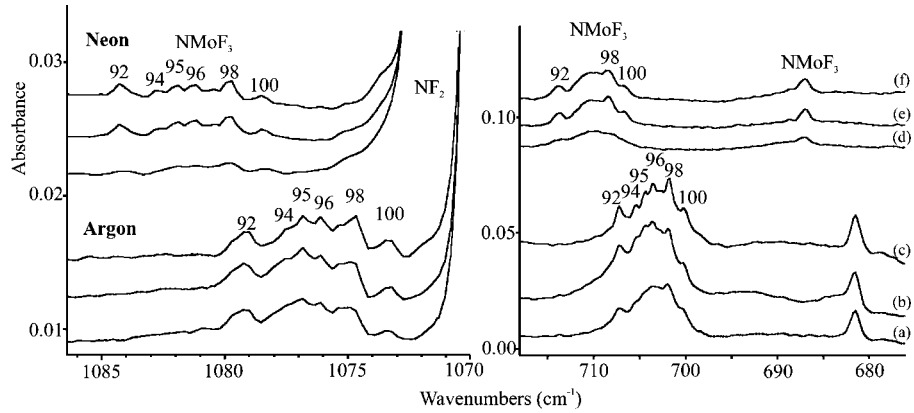

Figure 2. Infrared spectra for natural Mo atom reaction product with NF_3 in the 1080−1070 and 720−670 cm^{-1} regions using expanded wavenumber scale: (a) spectrum after codeposition of laser-ablated Mo and NF_3 at 0.4% in argon at 4 K for 60 min, (b) after > 220 nm irradiation for 20 min, and (c) after annealing to 25 K; (d) spectrum after codeposition of laser-ablated Mo and NF_3 at 0.2% in neon at 4 K for 60 min, (e) after 240−380 nm irradiation, and (f) after annealing to 8 K. Numbers denote molybdenum isotopic peaks.

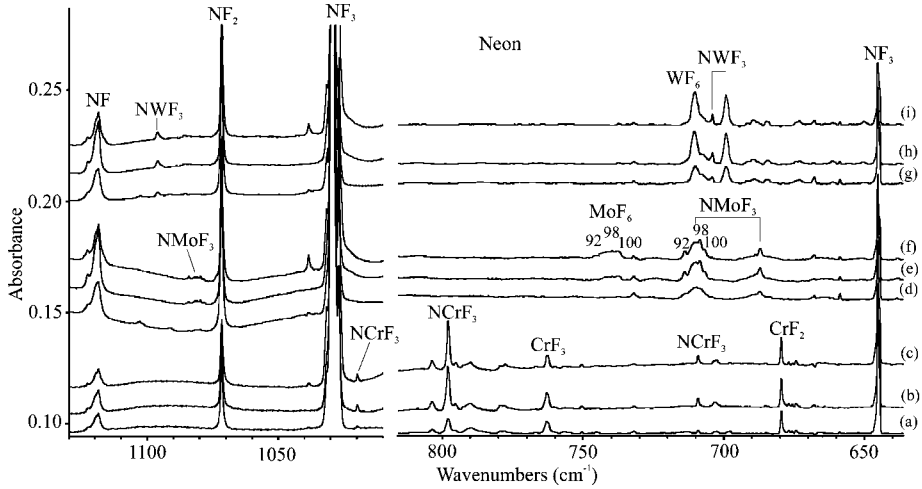

Figure 3. Infrared spectra for group 6 metal atom reaction products with NF_3 in excess neon in the 1130–1010 and 815–635 cm^{-1} regions: (a) spectrum after codeposition of laser-ablated Cr and NF_3 at 0.2% in neon at 4 K for 60 min, (b) after 240−380 nm irradiation for 20 min, and (c) after annealing to 8 K; (d) spectrum after codeposition of laser-ablated Mo and NF_3 at 0.2% in neon at 4 K for 60 min, (e) after 240−380 nm irradiation, and (f) after annealing to 8 K; (g) spectrum after codeposition of laser-ablated W and NF_3 at 0.2% in neon at 4 K for 60 min, (h) after 240−380 nm irradiation for 20 min, and (i) after annealing to 8 K.

and annealing, and this band is appropriate for MoF_6.[33,34] Molybdenum isotopic structure on the 1075 cm^{-1} band at 1079.1, 1077.5, 1076.8 1076.1, 1074.7 and 1073.4 cm^{-1} and on the 704 cm^{-1} band at 707.3, 705.5, 704.4, 701.8 and 700.2 cm^{-1} is amplified in Figure 2. For tungsten, a sharp 1091.1 cm^{-1} band and stronger 699.2 and 693.4 cm^{-1} absorptions increased on UV irradiation and decreased on annealing again in concert. A weak 706.7 cm^{-1} band increases more on irradiation and annealing and this band is due to WF_6, based on the high resolution band position of 713.9 cm^{-1} for $^{184}WF_6$.[34,35] Based on our calculations the new 607.5, 603.4 cm^{-1} band is probably due to WF_4.

Corresponding experiments were also performed in excess neon, and the spectra are compared in Figure 3. The NF_2 radical absorptions at 1071.6 and 936.1 cm^{-1} are between the argon matrix and gas phase values as is NF absorption at 1118.8 cm^{-1}.[31,36] The chromium studies produced new bands at 1019.8, 798.2 and 709.1 cm^{-1}, and the CrF_2 and CrF_3 absorptions shifted to 679.5 and 762.7 cm^{-1}. The Mo investigation revealed even better resolved Mo isotopic bands at 1080 and 708 cm^{-1} with components given in Table S1. The sharper band was observed at 687.0 cm^{-1}. The MoF_6 band at 740 cm^{-1} also revealed the Mo isotopic profile. The tungsten experiment in neon gave shifted bands at 1096.1, 710.2 (WF_6), 704.0, and 699.1 cm^{-1}.

PF_3. Reactions with laser-ablated Cr, Mo, and W atoms and PF_3 in excess argon gave the product spectra shown in Figure 4 and listed in Table 2. Two groups of common photosensitive bands (labeled PF_3^-) at 741 and at 465 cm^{-1} have been identified previously.[31] Weak bands at 638.7 and 760.5 cm^{-1} decreased on near-ultraviolet photolysis and increased on annealing. A 647.8 cm^{-1} band increased on UV irradiation and is probably due to CrF, based on the gas phase[37] fundamental at 655.7 cm^{-1}, and other bands with similar behavior are identified as CrF_2 and CrF_3 from previous work.[32]

Two absorptions were found with Mo, a broad band at 684 cm^{-1} with molybdenum isotopic splittings and a sharp feature at 662.2 cm^{-1}. Tungsten gave two sharp bands at 683.4 and 680.6 cm^{-1}, which increased 60% on UV > 220 nm irradiation, and decreased on annealing into sharper, completely resolved bands.

Analogous experiments were done using excess neon, and the spectra are compared in Figure 5. The bands shifted to higher wavenumbers (Table 2) are slightly stronger and their photochemical increases are similar to that observed in solid argon.

PCl_3. Laser-ablated Mo, and W atoms react with PCl_3 to give a product with weak absorptions at 436 and 416 cm^{-1}, respectively, in solid argon, which were little affected by sample irradiation and annealing. These bands are listed in Table 3.

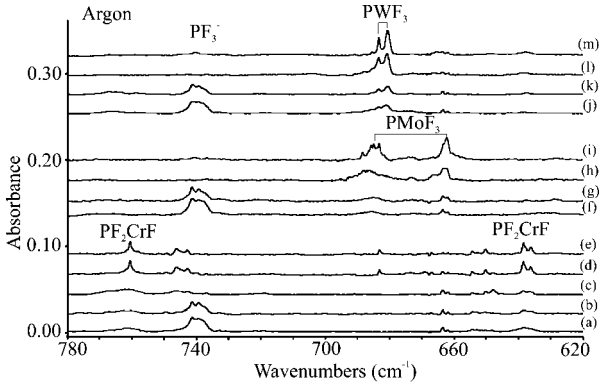

Figure 4. Infrared spectra for group 6 metal atom reaction products with PF_3 in excess argon in the 780−620 cm^{-1} region: (a) spectrum after codeposition of laser-ablated Cr and PF_3 at 0.5% in argon at 4 K for 60 min, (b) after annealing to 20 K, (c) after > 220 nm irradiation for 20 min, (d) after annealing to 30 K, and (e) after annealing to 35 K; (f) spectrum after codeposition of laser-ablated Mo and PF_3 at 0.5% in argon at 4 K for 60 min, (g) after annealing to 20 K, (h) after > 220 nm irradiation, and (i) after annealing to 30 K; (j) spectrum after codeposition of laser-ablated W and PF_3 at 0.5% in argon at 4 K for 60 min, (k) after annealing to 20 K, (l) after > 220 nm irradiation for 20 min, and (m) after annealing to 30 K.

N≡MF$_3$ Molecules. The major products in these experiments are identified as terminal metal nitrides from comparison between calculated and observed frequencies as outlined in Table 1. First, following our work with tri- and tetrahalomethanes,[18] these reactions proceed through insertion and fluorine transfer steps as outlined in reaction 1, which are even more exothermic for NF_3 than for CF_4. The energy profiles in Figure 6 show that reaction 1 is exothermic by 182, 298 and 328 kcal/mol for Cr, Mo, and W, respectively,

$$M + NF_3 \rightarrow NF_2{-}MF \rightarrow NF{=}MF_2 \rightarrow N{\equiv}MF_3 \qquad (1)$$

and that the terminal nitrides are the lowest energy species for this stoichiometry. Hence, the terminal nitride is the most favorable product in these reactions. Attempts to compute the M:NF_3 complex led directly to the NF_2−MF insertion product.

Figure 1 reveals weak bands at 1015, 1075, and 1091 cm^{-1}, respectively, for the group 6 metal products, which are in the region for terminal metal−nitride vibrations.[38,39] The resolution of six Mo isotopic components with relative intensities appropriate to the natural isotopic abundance confirms that a single Mo atom contributes to this vibration and the magnitude of the shift reveals the approximate mass of the vibrating partner.

Our resolution of natural isotopic molybdenum isotopic splittings on the 1075 cm^{-1} band is significant for several reasons. The relative intensities of the six-peak pattern in Figure 2 correspond with the statistical distribution of Mo isotopes in natural abundance. This demonstrates that a single Mo atom is involved in the vibrational mode, and it shows that the product molecule is cleanly isolated in the matrix. Next the magnitude of the Mo isotopic shift can be compared with that for other molecules to characterize the new vibrational mode. Molybdenum nitride is the most investigated second-row transition metal nitride. The gas phase frequencies for the most abundant ^{98}MoN and lightest ^{92}MoN molecules are 1044.7 and 1049.6 cm^{-1}, respectively.[40] This shift for the pure diatomic molecule vibration, 4.9 cm^{-1}, can be compared with the 4.4 and 4.5 cm^{-1} separations between the Mo 92 and 98 isotopic peaks in the argon and neon matrix N≡MoF_3 spectra (Figure 2). This indicates that Mo is vibrating less between N and three F and that N is moving slightly more than in the diatomic Mo≡N molecule, which confirms the assignment to a terminal Mo≡N vibrational mode. A similar normal mode was found for the Mo≡C stretching mode at 982.0−978.1 cm^{-1} for the analogous HC≡MoF_3 molecule.[18b] In contrast, the 1091 cm^{-1} N≡WF_3 counterpart is much sharper because the heavier tungsten isotopic profile is contained in the bandwidth, and the sharp 1015 cm^{-1} N≡CrF_3 band is for the major ^{52}Cr isotope. Our BPW91 calculation predicts the Mo-92 to 98 isotopic shift of the Mo≡N stretching mode within 0.1 cm^{-1} of the value observed for N≡MoF_3 in both solid argon and neon.

The two other associated argon matrix N≡MoF_3 bands at 704 and 682 cm^{-1} are broad and sharp, respectively. The breadth of the former conceals Mo isotopic splittings that are absent for the latter. Our calculation for these two antisymmetric and symmetric Mo−F stretching modes predicts 5.5 and 0.8 cm^{-1} Mo-92 to Mo-98 splittings and the argon matrix 704 cm^{-1} band is resolved to give a 5.4 cm^{-1} splitting and the neon matrix 708 cm^{-1} band is resolved to reveal a 5.5 cm^{-1} separation for these subpeaks (see Table S1). In contrast the 682 and 687 cm^{-1} bands have 1.0 cm^{-1} full widths at half-maximum, and our calculation is in accord with this isotopic profile. In the N≡MoF_3 molecule, the symmetric Mo−F stretching mode requires little Mo motion, whereas the antisymmetric motion involves Mo almost as much as in MoF_6 itself, which exhibits a corresponding 6.2 cm^{-1} splitting (Table S1).[33] Finally, the small 4−5 cm^{-1} blue shifts in these three bands on going from the argon to neon matrix environment reveals a stable molecule with minimal matrix interaction.

The sharp 1091.1, 699.2, and 693.4 cm^{-1} argon matrix and 1096.1, 704.0 and 699.1 cm^{-1} neon matrix bands are assigned to the W≡N, symmetric W−F and antisymmetric W−F stretching modes, respectively, of N≡WF_3. The correlation of theses observed frequencies with those calculated by two density functionals and the rigorous CASSCF/CASPT2 wave function based method (Table 1) confirm our assignments.

The strongest Cr product band at 791.9 cm^{-1} in solid argon shifts to 798.1 cm^{-1} in solid neon. These bands are due to the antisymmetric Cr−F motion of a new species. Our calculations for N≡CrF_3 predict a much weaker symmetric Cr−F mode 73−91 cm^{-1} lower and the weak 704.7 and 709.1 cm^{-1} argon and neon matrix bands are 87−89 cm^{-1} lower and appropriate for this assignment. The DFT calculations predict the Cr≡N mode much higher than does the CASSCF, and the latter is the more accurate predictor as it is 20 and 11 cm^{-1} higher for the Mo and W species in solid argon and 15 and 6 cm^{-1} higher than the corresponding solid neon observations. Thus the 1015 and 1020 cm^{-1} argon and neon matrix bands, which track with the stronger Cr−F modes (Figures 1 and 3), are due to the important diagnostic Cr≡N bond stretching mode. We find the terminal nitride to be 79 and 36 kcal/mol more stable than the first and second products of reaction (1) for chromium, and thus the favored product. The observed frequencies correlate well with the calculated frequencies (Table 1) and support this preparation of N≡CrF_3.

We have thus identified the three terminal nitrides N≡CrF_3, N≡MoF_3, and N≡WF_3 from their argon and neon matrix infrared spectra containing the M≡N and two M−F stretching modes and three different calculations of the strongest infrared vibrational frequencies as summarized in Table 1.

The observation of MoF_6 and WF_6 in these experiments and their increase on UV irradiation invites consideration of a favorable reaction mechanism. Reaction of the terminal nitrides with NF_3 itself to eliminate dinitrogen is in fact highly

TABLE 2: Observed and Calculated Vibrational Frequencies of the Group 6 P≡MF_3 Molecules in Singlet Ground Electronic States with C_{3v} Structures[a]

approximate	P≡CrF_3							P≡MoF_3							P≡WF_3						
description	obs[b]	cal(L)	int	cal(W)	int	cal(C)	int	obs[b]	Cal(L)	int	cal(W)	int	cal(C)	int	obs[b]	cal(L)	int	cal(W)	int	cal(C)	int
M−F, e	n. o.	762	306	753	260	796	460	686	690	294	680	256	706	416	681	675	242	665	214	696	322
M−F, a_1		716	110	693	94	729	168	662	664	113	649	93	688	160	683	672	96	659	79	697	141
M≡P, a_1		604	5	576	1	491	4		600	1	577	2	549	40		581	8	559	8	549	6
F−M−F, e		238	0	236	0	228	0		220	0	216	2	223	0		219	0	215	0	218	0
F−M−F, a_1		249	3	243	2	243	33		217	4	212	3	230	15		215	3	211	2	221	8
N−M−F, e		197	10	196	8	198	20		173	14	172	12	170	28		168	14	168	10	164	22

[a] Frequencies and intensities are in cm^{-1} and km/mol. Frequencies and intensities computed with B3LYP(L), BPW91(W), or CASSCF/CASPT2(C) methods in the harmonic approximation. Symmetry notations are for C_{3v} symmetry. [b] Observed in an argon matrix: the instrumental limit is 410 cm^{-1}. Neon matrix counterparts are (Cr) n. o., (Mo) 693, 671 cm^{-1}, and (W) 691, 688 cm^{-1}.

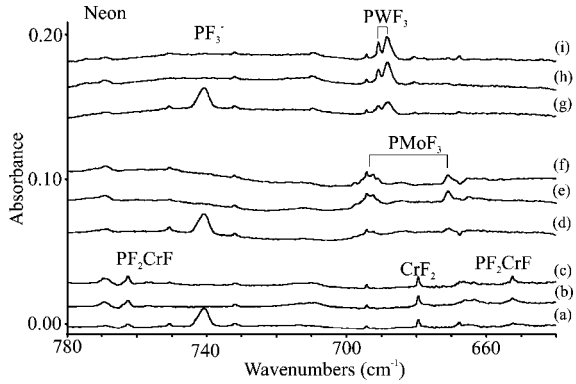

Figure 5. Infrared spectra for group 6 metal atom reaction products with PF_3 in excess neon in the 780−640 cm^{-1} region: (a) spectrum after codeposition of laser-ablated Cr and PF_3 at 0.2% in neon at 4 K for 60 min, (b) after 240−380 nm irradiation for 20 min, (c) after annealing to 8 K; (d) spectrum after codeposition of laser-ablated Mo and PF_3 at 0.2% in neon at 4 K for 60 min, (e) after 240−380 nm irradiation, and (f) after annealing to 8 K; (g) spectrum after codeposition of laser-ablated W and PF_3 at 0.2% in neon at 4 K for 60 min, (h) after 240−380 nm irradiation for 20 min, and (i) after annealing to 8 K.

exothermic (reaction energy −168 and −208 kcal/mol, respectively) for Mo and W, reaction 2.

$$F_3N + N{\equiv}MF_3 \rightarrow N{\equiv}N + MF_6 \qquad (2)$$

P≡MF_3 Molecules. The P≡MF_3 molecule has stronger bonds and the reaction energetics are different than found for NF_3. Reaction 3 is exothermic by 117 and 79 kcal/mol for W

$$M + PF_3 \rightarrow PF_2{-}MF \rightarrow PF{=}MF_2 \rightarrow P{\equiv}MF_3 \qquad (3)$$

and Mo, but endothermic by 12 kcal/mol for Cr, and PF_2−CrF is the lowest energy product (Figure 6, B3LYP energies). This relationship is manifest in the product identifications. Comparison of the spectra for the nitrides and phosphides of common metals reveals W−F stretching frequencies lower by 13−16 cm^{-1} for and Mo−F frequencies lower by 20 cm^{-1} for phosphides. The major absorptions for the Cr product appear at 638.7 and 760.5 cm^{-1} in solid argon and at 652.6 and 769.8 cm^{-1} in solid neon. As our calculations (Tables 1 and 2) do predict the strong (e) Cr−F mode of P≡CrF_3 to be 37 cm^{-1} lower than that for N≡CrF_3, the higher band could, in principle, be so assigned, but the weak (a_1) band is predicted 4 cm^{-1} lower and observed 66 cm^{-1} lower. Such is not compatible with this identification, nor is the much higher energy of the P≡CrF_3 molecule relative to other products. These absorptions do not fit the spectrum calculated for PF=CrF_2 (Table S2), but the strongest absorptions predicted for PF_2−CrF at 661 and 789 cm^{-1} correlate well with the observed bands. The higher band is in fact an antisymmetric PF_2 stretching mode and the lower band the Cr−F stretching mode.

On the other hand, the P≡MoF_3 and P≡WF_3 molecules are the most stable products and the observed bands in each case can be assigned to the symmetric M−F and antisymmetric M−F stretching modes. In the Mo case partially resolved Mo isotopic structure (Figures 4 and 5 and Table S1) demonstrate again the participation of a single Mo atom. The magnitude of the Mo 92−100 shift for the antisymmetric stretch (6.7 and 6.9 cm^{-1} in solid argon and neon) is almost the same as that found for N≡MoF_3 and just less than for MoF_6 in the gas phase (Table S1). And as for the nitride, the symmetric Mo−F stretching mode involves relatively little Mo motion and the band is sharp without metal isotopic broadening. Both absorptions are sharp for P≡WF_3 as the natural tungsten isotopic shifts are too small to be resolved here, and the band positions are well predicted by the calculations (Table 2).

In contrast no metal hexafluorides were observed in the reactions with PF_3. Even the most favorable reaction in the tungsten system is endothermic (+4 kcal/mol) so reaction 4 does not participate in these experiments.

$$F_3P + P{\equiv}MF_3 \not\rightarrow P{\equiv}P + MF_6 \qquad (4)$$

P≡MCl_3 Molecules. Following the favorable reactions of Mo and W atoms with PF_3 to form stable terminal phosphides, the analogous stable P≡$MoCl_3$ and P≡WCl_3 molecules were computed and found to be 116 and 157 kcal/mol lower in energy than the reagents. This shows that these P≡MCl_3 molecules are anticipated products. Our observation of the strongest IR absorptions for these P≡MCl_3 molecules (Table 3) supports this conclusion. Structures computed at the B3LYP level found shorter M≡P bonds by 0.003 and 0.002 Å, respectively, in the trichlorides than in the trifluorides.

Calculated Frequencies. Tables 1 and 2 provide a comparison of observed and calculated frequencies using three quantum chemical methods, the simpler hybrid and pure density functionals, and the more rigorous CASSCF/CASPT2 wave function approach, and several trends emerge. For the M−F stretching modes, the B3LYP frequencies are higher than the BPW91 values, as observed traditionally,[17,41] but the CASSCF/CASPT2 are higher still. On the other hand, the density functional methods overestimate the M≡N stretching frequencies, particularly the Cr≡N mode, whereas the CASSCF/CASPT2 method gives lower frequencies, only 1.1, 1.5, and 0.5% higher than the neon matrix values, which are expected to be closer to the unknown gas phase frequencies than the argon matrix observations.[42] The more rigorous method does particularly well here for describing the most complicated bond, the metal−nitrogen triple bond. However, the more rigorous method tends to overestimate the M−F stretching modes more than the B3LYP

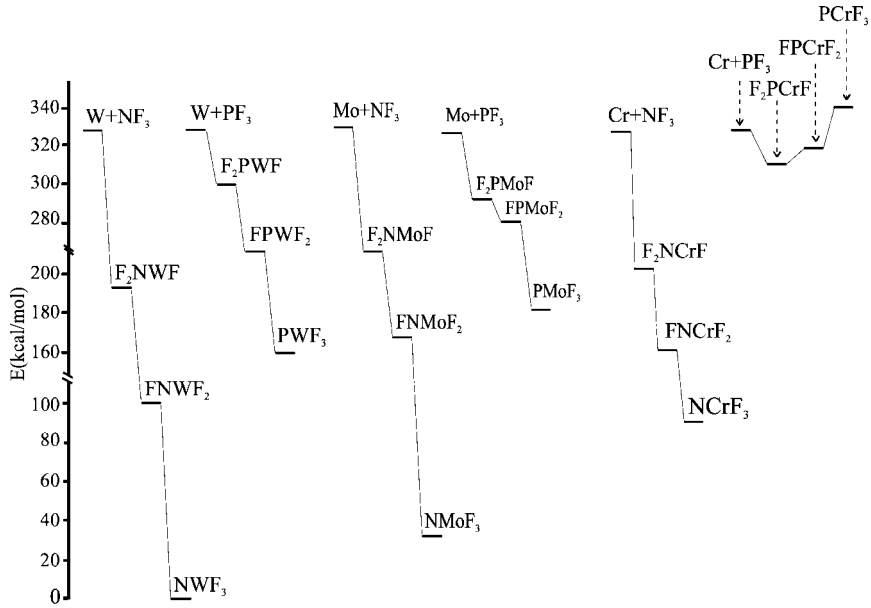

Figure 6. Energy profile of group 6 metal atom and NF_3 or PF_3 reaction products computed at the B3LYP level of theory relative to the energy of the metal atom and the reagent molecule.

TABLE 3: Observed and Calculated Frequencies of the P≡MoCl$_3$ and P≡WCl$_3$ Molecules in the Singlet Ground Electronic States with C_{3v} Structures[a]

approximate description	P≡MoCl$_3$			P≡WCl$_3$		
	obs	cal(L)	int	obs	cal(L)	int
M−Cl str, a_1		599	11		574	8
M−Cl str, e	436	423	160	416	400	132
M≡P str, a_1		381	17		388	18
Cl−M−Cl bend, e		172	2		169	0
Cl−M−Cl bend, a_1		141	0		135	0
Cl−M−Cl bend, e		103	0		101	0

[a] Frequencies and intensities are in cm^{-1} and km/mol. Observed in an argon matrix. Frequencies and intensities computed with B3LYP(L) method in the harmonic approximation. Symmetry notations are for C_{3v}.

functional, and often the BPW91 functional underestimates these modes. It is also noteworthy that both functionals underestimate the W−F modes, and for this more electron rich molecule, the CASSCF/CASPT2 method is clearly superior. Finally, the calculation of frequencies for complicated molecules like these containing transition metals and multiple bonds is not an exact science, and the coverage obtained with several methods provides confidence that the calculated and observed frequencies are converging on the truth.

Structures. The C_{3v} structures computed for terminal nitride and phosphide trifluoride complexes are illustrated in Figure 7, and parameters are given for three theoretical methods, where the CASSCF/CASPT2 (bold type) is expected to be the most accurate. We also find C_{3v} structures and virtually the same computed terminal nitride bond lengths for the analogous trihydride species prepared from ammonia.[43] These values are compared in Table 4 along with bond orders and Mulliken charges. One might expect the W≡N bond to be much longer than the Mo≡N bond, but the difference is only 0.034 Å. The W and Mo ions have similar sizes. This is again illustrated by the M−F bond distances, which differ by only 0.011 Å. The weaker bonding in the phosphorus compounds manifests itself in longer M≡P bond distances where the Mo and W species are again very similar.

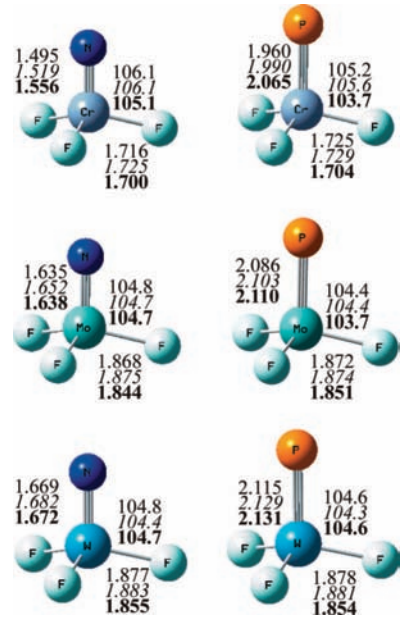

Figure 7. Structures calculated for the group 6 E≡MF$_3$ molecules in C_{3v} symmetry using B3LYP, BPW91 (italic values), and CASSCF/CASPT2 (bold values) methods with parameters given for each method, respectively.

Our calculated parameters can be compared to measurements of such bonds in larger organometallic complexes. Computations for the present simple complex Mo≡N and Mo≡P bond lengths are in agreement within error of measurement and calculation for larger representative organometallic complexes, 1.634 Å and 2.114 Å, respectively.[44,45] Likewise, terminal W≡N and W≡P bond lengths of 1.669 and 2.119 Å in analogous complexes[46,47] are essentially in agreement with those calculated for the present simple ternary complexes (Figure 7). A recent density functional theoretical bonding analysis of (MeO)$_3$W≡N and (MeO)$_3$W≡P complexes finds 1.665 and 2.118 Å bond lengths, which are almost the same, and triple bond σ and π components which are slightly larger, than the CASSCF/CASPT2 values reported here for the N≡WF$_3$ and P≡WF$_3$ molecules.[48] A comparison of the Mo counterparts for both finds the same relationship.

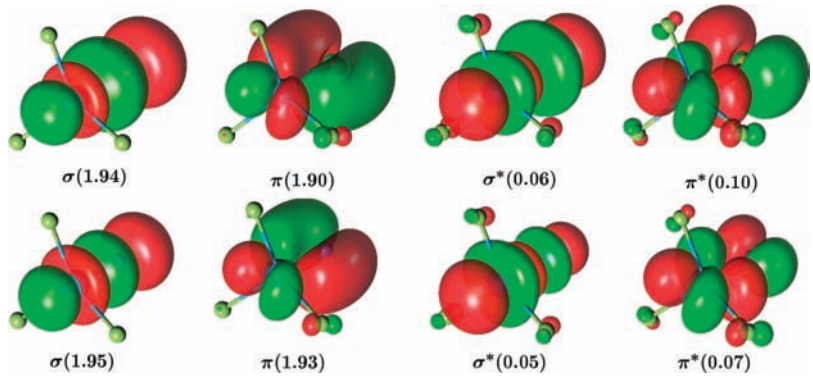

Figure 8. Active bonding and antibonding molecular orbitals for the P≡WF_3 (top row) and N≡WF_3 (bottom row) molecules. The contour line used is 0.05 e/au^3. Natural orbital occupation numbers are given below each orbital (only one component of the pi orbitals is shown).

TABLE 4: CASPT2 Geometry Parameters for E≡MF_3 Molecules in C_{3v} Symmetry (Bond Distances in Angstroms and Angles in Degrees)[a]

	N≡CrF_3	N≡MoF_3	N≡WF_3	P≡CrF_3	P≡MoF_3	P≡WF_3
R(E≡M)	1.556	1.638	1.672	2.065	2.110	2.131
R(M−F)	1.700	1.844	1.855	1.704	1.851	1.854
<EMF	105.1	104.7	104.7	103.7	103.7	104.6
<FMF	113.4	113.7	113.8	114.5	114.6	113.8
energy	76	135	155	39	73	103
EBO	2.59	2.77	2.80	2.18	2.67	2.74
X charge	−0.14	−0.40	−0.43	0.25	−0.10	−0.01
M charge	1.75	2.18	2.24	1.56	1.92	1.80

[a] Computed bond energies in kcal/mol and effective bond orders (EBO) for the E≡M bond are also shown together with the Mulliken charges for the E and M atoms.

TABLE 5: Natural Orbital Occupation Numbers for E≡MF_3 Molecules and the Resulting Effective Bond Order (EBO)[a]

molecule	σ	π	σ^*	π^*	EBO
N≡CrF_3	1.90	3.69	0.10	0.31	2.59
N≡MoF_3	1.94	3.83	0.06	0.17	2.77
N≡WF_3	1.95	3.85	0.05	0.15	2.80
HC≡WF_3	1.96	3.84	0.04	0.16	2.80
P≡CrF_3	1.85	3.34	0.15	0.66	2.18
P≡MoF_3	1.93	3.74	0.07	0.26	2.67
P≡WF_3	1.94	3.79	0.06	0.21	2.74

[a] Values for π orbitals summed over both components. (12 in 12) used for N≡CrF_3.

Finally, our computed nitrogen triple bond lengths for Mo and W are about 2% shorter than those taken from tabulated triple bond radii[49] whereas our computed phosphorus triple bond lengths are about 2% longer.

Bonding in Terminal Nitride and Phosphide Complexes. The rigorous CASSCF/CASPT2 method has been employed to analyze the bonding in these simple ternary pnictide complexes. The molecular orbitals are illustrated for the N≡WF_3 and P≡WF_3 complexes in Figure 8, and Table 5 compares the σ and π components for the analogous Mo and Cr complexes. The effective bond order (EBO) is computed as the difference between the occupation numbers of the bonding and antibonding orbitals divided by 2. Several trends are found in Table 5. The increase in EBO on going down the family group is composed of an increase in the bonding and a decrease in the antibonding orbital occupations, which follows the increase in stability of the highest oxidation state. Natural bond orders are slightly smaller for the phosphide than the corresponding nitride complexes, and the difference between N and P is most pronounced for Cr as the diffuse 3p orbitals of P do not bind well with the very compact 3d orbitals of Cr whereas the more compact 2p orbitals of N bond a little better. The triple bond order follows the bond polarity as the metal valence electrons are shared with the nonmetal to form the triple bond. The 2.59, 2.77, and 2.80 bond orders for the N≡CrF_3, N≡MoF_3, and N≡WF_3 series have about the same relationship as those for the hextuply bonded dimers Cr_2, Mo_2, and W_2 (3.5, 5.2, and 5.2).[50] Finally, note that the M≡N stretching frequency increases with the M≡N bond order.

It is also of interest to compare the energy of the triple bond for the three transition metals to the smaller two group 15 elements, which has been computed at the CASSCF/CASPT2 level as the energy of reaction 5. The MF_3 molecules were assumed

$$E + MF_3 \rightarrow E{\equiv}MF_3 \quad (5)$$

to be planar with D_{3h} symmetry and the M−F bond distance was optimized. The resulting energies do not include ZPE correction or spin−orbit coupling and are therefore not very accurate. However, they illustrate nicely the trends in the bond strength discussed above. The bond energies follow the same trends given by the bond orders (Table 4). The bond energy increases in the series Cr−Mo−W. The phosphorus−metal bond is considerably weaker than the nitrogen−metal bond. This is particularly evident for the P≡Cr bond. For nitrogen these triple bond energies increase (76, 135, 155 kcal/mol) going down the group 6 family, and for phosphorus the triple bond energies increase (39, 73, 103 kcal/mol).

Conclusions

Group 6 metal atoms react with NF_3 and PF_3 upon excitation by laser ablation or UV irradiation to form stable trigonal E≡MF_3 pnictide molecules with the exception of P≡CrF_3, which is too high in energy to compete with the first step in the reaction, namely PF_2−CrF. These molecules are identified by comparison of closely related and mutually reinforcing argon and neon matrix infrared spectra with frequencies calculated by three theoretical methods. The natural bond orders computed by CASSCF/CASPT2 increase from 2.59 to 2.77 to 2.80 in the N≡CrF_3 to N≡MoF_3 to N≡WF_3 series as the metal orbital size becomes more compatible with nitrogen valence orbitals and the higher oxidation state more stable. And as a direct consequence, the Cr≡N, Mo≡N, and W≡N stretching frequencies increase going down the family group. The corresponding bond orders for P≡CrF_3, P≡MoF_3, and P≡WF_3 are 2.18, 2.67, and 2.74. Hence, the group 6 metal phosphide bond orders are

less than the corresponding nitrides as expected for the larger phosphorus valence orbitals.

Acknowledgment. We gratefully acknowledge financial support from NSF Grant CHE 03-52487 and NCSA computing Grant No. CHE07-0004N to L.A. and from the Swedish Research Council (VR) through the Linnaeus Center of Excellence on Organizing Molecular Matter (OMM) to R.L. and B.O.R.

Supporting Information Available: Complete ref 21 and Tables S1 and S2 containing molybdenum isotopic frequencies and calculated phosphorus intermediate species frequencies, respectively. This material is available free of charge via the Internet at http://pubs.acs.org.

References and Notes

(1) (a) Dehnicke, K.; Strähle, J. *Angew. Chem., Int. Ed. Engl.* **1992**, *31*, 955. (b) See also: Dehnicke, K.; Weller, F.; Strähle, J. *Chem. Soc. Rev.* **2001**, *30*, 125.

(2) Balazs, G.; Gregoriades, L. J.; Scheer, M. *Organometallics* **2007**, *26*, 3058.

(3) Gdula, R. L.; Johnson, M. J. A.; Ockwig, N. W. *Inorg. Chem.* **2005**, *44*, 9140.

(4) Gdula, R. L.; Wiedner, E. S.; Johnson, M. J. A. *J. Am. Chem. Soc.* **2006**, *128*, 9614.

(5) Geyer, A. M.; Gdula, R. L.; Wiedner, E. S.; Johnson, M. J. A. *J. Am. Chem. Soc.* **2007**, *129*, 3900.

(6) Chisholm, M. H.; Hoffman, D. M.; Juffnan, J. C. *Inorg. Chem.* **1983**, *22*, 2903.

(7) Close, M. R.; McCarley, R. E. *Inorg. Chem.* **1994**, *33*, 4198.

(8) Laplaza, C. E.; Davis, W. M.; Cummins, C. C. *Angew. Chem., Int. Ed. Engl.* **1995**, *34*, 2042–2044.

(9) Cherry, J. P. F.; Stephens, F. H.; Johnson, M. J. A.; Diaconescu, P. L.; Cummins, C. C. *Inorg. Chem.* **2001**, *40*, 6860–6862.

(10) Stephens, F. H.; Figueroa, J. S.; Diaconescu, P. L.; Cummins, C. C. *J. Am. Chem. Soc.* **2003**, *125*, 9264–9265.

(11) Figueroa, J. S.; Cummins, C. C. *J. Am. Chem. Soc.* **2004**, *126*, 13916.

(12) Fox, A. R.; Clough, C. R.; Piro, N. A.; Cummins, C. C. *Angew. Chem., Int. Ed.* **2007**, *46*, 973–976.

(13) Odom, A. L.; Cummins, C. C.; Protasiewicz, J. D. *J. Am. Chem. Soc.* **1995**, *117*, 6613–6614.

(14) Odom, A. L.; Cummins, C. C. *Polyhedron* **1998**, *17*, 675–688.

(15) Odom, A. L.; Cummins, C. C. *Organometallics* **1996**, *15*, 898–900.

(16) Schrock, R. R. *Chem. Rev.* **2002**, *102*, 145 (Review article).(17) Andrews, L.; Cho, H.-G. *Organometallics* **2006**, *25*, 4040, and references therein (Review article).(18) (a) Lyon, J. T.; Andrews, L. *Organometallics* **2007**, *26*, 2519. (b) Lyon, J. T.; Cho, H.-G.; Andrews, L. *Organometallics* **2007**, *26*, 6373. (19) Andrews, L.; Citra, A. *Chem. Rev.* **2002**, *102*, 885, and references therein. (20) Andrews, L. *Chem. Soc. Rev.* **2004**, *33*, 123, and references therein. (21) Kudin, K. N.; et al. *Gaussian 03*, revision D.01, Gaussian, Inc.: Pittsburgh, PA, 2004.(22) (a) Becke, A. D. *J. Chem. Phys.* **1993**, *98*, 5648. (b) Lee, C.; Yang, Y.; Parr, R. G. *Phys. Rev. B* **1988**, *37*, 785. (23) Frisch, M. J.; Pople, J. A.; Binkley, J. S. *J. Chem. Phys.* **1984**, *80*, 3265. (24) Andrae, D.; Haeussermann, U.; Dolg, M.; Stoll, H.; Preuss, H. *Theor. Chim. Acta.* **1990**, *77*, 123. (25) Roos, B. O. *The Complete Active Space Self-Consistent Field Method and its Applications in Electronic Structure Calculations, in Advances in Chemical Physics; Ab Initio Methods in Quantum Chemistry - {II}*; Lawley, K. P. Ed.; John Wiley & Sons Ltd.: New York, 1987; p 399.(26) Andersson, K.; Malmqvist, P.-Å.; Roos, B. O. *J. Chem. Phys.* **1992**, *96*, 1218. (27) Roos, B. O.; Lindh, R.; Malmqvist, P.-Å.; Veryazov, V.; Widmark, P.-O. *J. Phys. Chem. A* **2004**, *108*, 2851. (28) Roos, B. O.; Lindh, R.; Malmqvist, P.-Å.; Veryazov, V.; Widmark, P.-O. *J. Phys. Chem. A* **2005**, *109*, 6575. (29) Roos, B. O.; Lindh, R.; Malmqvist, P.-Å.; Veryazov, V.; Widmark, P.-O. *Chem. Phys. Lett.* **2005**, *409*, 295. (30) Karlström, G.; Lindh, R.; Malmqvist, P.-Å.; Roos, B. O.; Ryde, U.; Veryazov, V.; Widmark, P.-O.; Cossi, M.; Schimmelpfennig, B.; Neogrady, P.; Seijo, L. *Comput. Mater. Sci.* **2003**, *28*, 222. (31) (a) Jacox, M. E. *J. Phys. Chem. Ref. Data* **1998**, *27* (2), 115. (b) Lugez, C. L.; Irikura, K. K.; Jacox, M. E. *J. Chem. Phys.* **1998**, *108*, 8381. (32) (a) Van Leirsburg, D. A.; DeKock, C. W. *J. Phys. Chem.* **1974**, *78*, 134. (b) Blinova, O. V.; Shklyarik, V. G.; Shcherlie, L. D. *Zh. Fiz. Khim.* **1988**, *62*, 1640 (CrF_2, CrF_3).(33) The strongest IR band for $^{98}MoF_6$ appears at 743.3 cm^{-1} in the gas phase and the Mo-92 to Mo-100 shift is 7.2 cm^{-1}, which predicts an unresolved bandwidth of 7.2 cm^{-1} for the band in solid argon. Our bands at 736.8, 734.9 cm^{-1} have the appropriate molybdenum isotopic contour. (a) Takami, M.; Matsumoto, Y. *Mol. Phys.* **1988**, *64*, 645 (MoF_6).(34) Osin, S. B.; Davlyatshin, D. I.; Ogden, J. S. *Zh. Fiz. Khim.* **2001**, *75*, 294. (35) The strongest IR band for $^{184}WF_6$ is 713.9 cm^{-1} in the gas phase, and the W-182 to W-186 shift is 1.3 cm^{-1}. (a) Boudon, V.; Rotger, M.; He, Y.; Hollenstein, H.; Quack, M.; Schmitt, U. *J. Chem. Phys.* **2002**, *117*, 3196 (WF_6).(36) Jacox, M. E.; Milligan, D. E. *J. Chem. Phys.* **1967**, *46*, 184. (37) Bencheikh, M.; Koivisto, R.; Launila, O.; Flament, J. P. *J. Chem. Phys.* **1997**, *106*, 6231. (38) Andrews, L. *J. Electron Spectrosc. Rel. Phen.* **1998**, *97*, 63. (39) Andrews, L.; Souter, P. F.; Bare, W. D.; Liang, B. *J. Phys. Chem. A* **1999**, *103*, 4649 (Mo, W + N_2).(40) Sze, N. S.-K.; Cheung, A.S.-C. *J. Quant. Spectrosc. Radiat. Transfer* **1994**, *52*, 145 (MoN gas phase).(41) (a) Scott, A. P.; Radom, L. *J. Phys. Chem.* **1996**, *100*, 16502. (b) Andersson, M. P.; Uvdal, P. L. *J. Phys. Chem. A* **2005**, *109*, 3937. (c) von Frantzius, G.; Streubel, R.; Brandhorst, K.; Grunenberg, J. *Organometallics* **2006**, *25*, 118. (42) Jacox, M. E. *Chem. Phys.* **1994**, *189*, 149. (43) Wang, X.; Andrews, L. *Organometallics* **2008**, in press (group 6 metals + ammonia).(44) Gebeyehu, Z.; Weller, B.; Neumuller, K.; Dehnicke, K. *Z. Anorg. Allg. Chem.* **1991**, *593*, 99 (R_3MoN bond lengths).(45) See ref 10 for R_3MoP bond lengths. (46) Clough, C. R.; Greco, J. B.; Figueroa, J. S.; Diaconescu, P. L.; Davis, W. M.; Cummins, C. C. *J. Am. Chem. Soc.* **2004**, *126*, 7742 (R_3WN bond lengths).(47) See ref 12 for R_3WP bond lengths. (48) Pandey, K. K.; Frenking, G. *Eur. J. Inorg. Chem.* **2004**, 4388. (49) Pyykko, P.; Riedel, S.; Patzschke, M. *Chem. Eur. J.* **2005**, *12*, 3511. (50) Roos, B. O.; Borin, A. C.; Gagliardi, L. *Angew. Chem., Int. Ed.* **2007**, *46*, 1469.

JP804469A